

## Scintigraphic distribution of complexes of antiinsulin antibodies and 123I-insulin. In vivo studies in rats.

F Sodoyez-Goffaux, ... , C J De Vos, R von Frenckell

*J Clin Invest.* 1987;**80**(2):466-474. <https://doi.org/10.1172/JCI113094>.

### Research Article

Clearance of immune complexes made of antiinsulin antibodies and 123I-insulin was studied with scintillation scanning in anesthetized rats. Complexes made with purified guinea pig antiinsulin IgG2 (cytophilic isotype) were rapidly cleared by the liver whereas those made with IgG1 remained in the plasma, as did 123I-labeled IgG1 or IgG2 of control animals. Hepatic clearance of insulin-antiinsulin IgG complexes was not inhibited by either an excess of insulin or decomplementation, thereby ruling out interaction with insulin and C3b receptors. Insulin and guinea pig antiinsulin serum or its purified IgG isotypes formed large aggregates exceeding 5 IgG. Antiinsulin antibodies of diabetics, mostly IgG1 and IgG3 (cytophilic isotypes), formed complexes that either remained in plasma (small aggregates) or were cleared by the liver (large aggregates). In conclusion, clearance of insulin-antiinsulin IgG complexes is probably mediated by Fc gamma receptors on macrophages and requires cytophilic subclass composition and formation of large IgG aggregates.

**Find the latest version:**

<https://jci.me/113094/pdf>



# Scintigraphic Distribution of Complexes of Antiinsulin Antibodies and $^{123}\text{I}$ -Insulin In Vivo Studies in Rats

Françoise Sodoyez-Goffaux, Jean-Claude Sodoyez, Michel Koch, Nicoletta Dozio, Edward R. Arquilla, Brenda McDougall, Claudine J. De Vos, and Remy von Frenckell  
Laboratory of Experimental Nuclear Medicine, University of Liège, B-4020 Liège, Belgium

## Abstract

Clearance of immune complexes made of antiinsulin antibodies and  $^{123}\text{I}$ -insulin was studied with scintillation scanning in anesthetized rats. Complexes made with purified guinea pig antiinsulin IgG2 (cytophilic isotype) were rapidly cleared by the liver whereas those made with IgG1 remained in the plasma, as did  $^{123}\text{I}$ -labeled IgG1 or IgG2 of control animals. Hepatic clearance of insulin-antiinsulin IgG complexes was not inhibited by either an excess of insulin or de complementation, thereby ruling out interaction with insulin and C3b receptors.

Insulin and guinea pig antiinsulin serum or its purified IgG isotypes formed large aggregates exceeding 5 IgG. Antiinsulin antibodies of diabetics, mostly IgG1 and IgG3 (cytophilic isotypes), formed complexes that either remained in plasma (small aggregates) or were cleared by the liver (large aggregates). In conclusion, clearance of insulin-antiinsulin IgG complexes is probably mediated by Fc $\gamma$  receptors on macrophages and requires cytophilic subclass composition and formation of large IgG aggregates.

## Introduction

Controversy has existed regarding the involvement of insulin antibodies in the clinical management of insulin-treated patients. Virtually all diabetic patients treated with insulin develop circulating antibodies, and these are now routinely detected by a variety of techniques (1-7).

As for all plasma components, antibody concentration is the result of equilibrium between antibody synthesis and clearance rates. The situation is probably more complex in diabetic patients because they daily receive one or several insulin (antigen) injection(s), and immune complexes made of insulin-antiinsulin antibodies are constantly formed. These immune complexes (IC)<sup>1</sup>

may be cleared at a higher rate than free antibodies and, as a consequence, the turnover rate of antiinsulin antibodies in the plasma compartment will be increased. In our opinion, too little attention has been paid to the dynamic aspect of this equilibrium, i.e., to the antibody "flux."

For instance, if IC are rapidly cleared from the plasma, an increase of daily insulin requirement matching the rate of IC clearance will allow a new steady state. In this instance, one might even expect that, if the antigen is in constant excess with regard to the antibodies, the plasma level of antibody could be low. By contrast, if the IC are slowly cleared from the plasma, little insulin will be scavenged by the macrophagic system and the daily insulin requirement should be expected to be almost normal, despite a potentially high level of plasma antibody. In this instance, if plasma antibody level is high, large amounts of insulin may be present in the plasma compartment, partly as antibody bound and partly as free (i.e., biologically active) hormone. The relative proportions between these two forms of insulin will depend on the avidity of the antibodies for their ligand. High-avidity antibodies will sequester their ligand in an almost nonreversible manner. By contrast low-avidity antibodies, normally in equilibrium in the presence of a high level of free insulin, will unduly release their ligand when insulin is not metabolically needed and are likely to cause hypoglycemic episodes between meals or at night.

Thus, antibodies will act as insulin scavengers and cause insulin-resistant diabetes or as carrier proteins and potentially cause unstable diabetes according to clearance rates of their IC. Several factors influence IC clearance rate, including IgG subclass and IC size. To our knowledge, there is little or no documented information on this subject with regard to insulin antibodies.

The method employed by this laboratory to measure the biokinetics of  $^{123}\text{I}$ -Tyr A14 monoiodoinsulin ( $^{123}\text{I}$ -ins) injected intravenously with a scintillation gamma camera connected to a computer has been described (8). In view of these considerations, we designed experiments employing this method to determine the effect of antiinsulin antibodies on the distribution and metabolism of preformed immune complexes containing  $^{123}\text{I}$ -insulin.

## Methods

**Labeled insulins.** Purified bovine insulin (0.1 mg; Novo, Copenhagen, Denmark) was labeled with Na  $^{123}\text{I}$  or Na  $^{125}\text{I}$  (5-10 mCi) and the species labeled on Tyr A14 was purified by reverse-phase HPLC (8-10).

**Guinea pig antiinsulin serum (GPAIS) pools and IgG fractions.** Guinea pig antiinsulin serum pool 469 was a generous gift of P. H. Wright (Indianapolis, IN). Other guinea pig insulin antiserum pools were

Presented in part at the Twelfth International Diabetes Federation Congress, Madrid, Spain, 1985, and published in abstract form (1985. *Diabetes Res. Clin. Pract. Suppl.* 1: S525a).

Address correspondence to Dr. Jean-Claude Sodoyez, Department of Internal Medicine, University of Liège, Hopital de Bavière, 66 Blvd. de la Constitution, B-4020 Liège, Belgium.

Part of this work was performed while E. R. Arquilla was on sabbatical leave from the Department of Pathology, University of California, Irvine.

Received for publication 27 January 1987.

1. **Abbreviations used in this paper:** AIIgG1 and AIIgG2, guinea pig antiinsulin IgG1 and IgG2; C3bR, receptors for C3b; CoF, cobra venom factor; Fc $\gamma$ R, receptors for Fc fragment of IgG; FPLC, fast protein liquid chromatography; GPAIS, guinea pig antiinsulin serum; HSA, human

J. Clin. Invest.

© The American Society for Clinical Investigation, Inc.

0021-9738/87/08/0466/09 \$2.00

Volume 80, August 1987, 466-474

serum albumin; IC, immune complexes;  $^{123}\text{I}$ -ins,  $^{123}\text{I}$ -Tyr A14-monoiodoinsulin; NIgG1 and NIgG2, IgG1 and IgG2 of noninsulin-immunized guinea pig; PEG, 25% polyethylene glycol.

obtained after hyperimmunization with bovine insulin as previously described (11).

The guinea pig antiinsulin IgG1 and IgG2 (AIIgG1 and AIIgG2) fractions were prepared from the same insulin antiserum pool by anion exchange chromatography (12). The IgG2 fraction gave a single slow migrating precipitin arc in the gamma globulin region by immunoelectrophoresis against rabbit anti-whole guinea pig serum. The IgG1 fraction gave one major arc in the gamma globulin region and two minor faster migrating precipitin arcs in the beta globulin region against the same rabbit anti-guinea pig serum.

The guinea pig IgG1 and IgG2 fractions contain very similar levels of insulin antibodies as determined by superimposable radioimmune titration and inhibition curves generated by a previously described method (13–15). In the absence of inhibitor, 0.1 ml of each fraction diluted 1:2,300 bound  $7.0 \times 10^3$  cpm  $^{125}\text{I}$ -ins. In the presence of 1 ng of bovine monocomponent insulin as inhibitor, 0.1 ml of each fraction at a dilution of 1:350 was required to bind  $7.0 \times 10^3$  cpm of the same  $^{125}\text{I}$ -ins preparation (Fig. 1). The AIIgG2 fraction induced passive immune hemolysis of insulin-coated sheep red blood cells (13) in the presence of excess guinea pig complement, whereas under identical conditions the AIIgG1 fraction did not. The AIIgG1 fraction was in 0.015 mol/liter phosphate, 9% NaCl, pH 7.4 (phosphate-buffered saline; PBS), at a protein concentration of 2.1 mg/ml. The AIIgG2 fraction was in the same solution at a protein concentration of 1.4 mg/ml. Both fractions were stored in aliquots at  $-20^\circ$  until used.

**Human antiinsulin serums.** Serum samples of insulin-immunized diabetic patients were characterized with regard to total antiinsulin IgG and antiinsulin IgG subclass composition by a recently reported solid-phase assay (16). Their avidity for bovine insulin was assayed by measuring the dissociation rate of preformed immune complexes. Briefly, serum samples were preincubated with  $^{125}\text{I}$ -insulin ( $4^\circ$  overnight), allowed to warm up to laboratory temperature, and mixed with activated charcoal suspension at time zero. The suspension was kept under vigorous magnetic stirring, and aliquot samples were drawn at selected times and centrifuged immediately to determine the percentage of activity in the pellet (dissociated insulin) and supernatant (antibody-bound insulin). In this assay, the  $T/2$  of preformed IC ranges from 10 min for low-avidity antibodies to several hours for high-avidity antibodies. The two serums selected displayed a high avidity for insulin. Their insulin binding activity was essentially carried out by IgG1 and IgG3, i.e., two cytophilic IgG isotypes, but they differed in size of IC made with insulin (Table I).

**Estimation of insulin-antiinsulin IC size.** Preformed IC made of purified AIIgG1, AIIgG2, or whole serum and  $^{125}\text{I}$ -ins were submitted to gel filtration on a  $60 \times 1.2$ -cm 6B Sepharose column equilibrated and developed with PBS containing 1% bovine serum albumin (BSA). Dextran blue, apoferritin (mol wt 449,000),  $\beta$  amylase (mol wt 200,000), guinea pig IgG (mol wt 160,000), and lysozyme (mol wt 14,300) served as markers and IC were detected by measuring radioactivity of the fractions. In control runs, purified AIIgG1, AIIgG2, and whole GPAIS were chro-

Table I. Properties of Human Antiinsulin Serums 1 and 2

	Serum 1	Serum 2
Serum concentration of antiinsulin IgG (ng equivalent myelomatous protein/ml)	60,124	3,412
Serum concentration of antiinsulin IgG subclasses (% of total)		
AIIgG1	79	100
AIIgG2	—	—
AIIgG3	20	—
AIIgG4	1	—
Half-life of IC (min)	170	240

matographed and antiinsulin antibodies were detected by measuring the  $^{125}\text{I}$ -ins binding capacity of each fraction.

As flow rate was 4 ml/h, 10 h were required for elution of IC. As discussed later, to minimize their dissociation during the process of chromatography, we also determined IC size by a faster technique, using Superose 6 and a fast protein liquid chromatography (FPLC) system (Pharmacia, Uppsala, Sweden) connected with an ultraviolet (UV) detector. The column was equilibrated and run with 120 mmol/liter phosphate, 1 mmol/liter EDTA, and 0.2 g/liter  $\text{NaN}_3$ , pH 7.4. Bovine thyroglobulin (mol wt 669,000), human IgG (mol wt 158,000), BSA (mol wt 60,000), and  $^{125}\text{I}$ -insulin were used as molecular weight markers to calibrate the column. The samples were eluted at 0.4 ml/min, and fractions of 200  $\mu\text{l}$  were collected. Absorbance at 280 nm was read by the online UV detector, and activity in each fraction was measured in a well-type counter.

**In vivo animal studies with preformed IC containing  $^{125}\text{I}$ -insulin.** Control rats received carrier-free  $^{125}\text{I}$ -ins ( $\sim 100 \mu\text{Ci}$ ) in  $\sim 0.5$  ml PBS containing 0.35% BSA. The experimental rats received  $^{125}\text{I}$ -ins ( $\sim 100 \mu\text{Ci}$  in 0.1 ml) mixed with AIIgG1 (0.4 ml), AIIgG2 (0.4 ml), human serum (1 ml), or whole GPAIS (40  $\mu\text{l}$  of pool 469 or 3F4 diluted 1:10 with PBS-albumin). Before injection, the various solutions were incubated at  $37^\circ$  for 30 min. Two experimental rats were pretreated with purified cobra venom factor (CoF; 80  $\mu\text{g}$ ), an activator of the alternative pathway of the complement, to minimize the level of circulating factors C3 to C9 (17). Another control group was pretreated with 6 U regular insulin to saturate the insulin receptor compartment.

$^{125}\text{I}$ -Ins alone or mixed with either purified guinea pig immunoglobulin fraction or whole antiinsulin serum was injected into the jugular vein of anesthetized (60 mg/kg Pentobarbital, i.p.), fed young female Sprague-Dawley rats weighing 225–275 g. The rats were laid prone on the high-resolution parallel collimator of a 400 T Maxi-Camera (General Electric Co., Milwaukee, WI) on-line with a Star computer system. Immediately after the injection, the data were recorded in a  $128 \times 128$  matrix at a rate of two frames per minute for a period of 30 min (dynamic study). Analogue scintigraphic images were also obtained at 3, 10, 20, and 30 min.

Immediately after the 30-min dynamic study, blood was drawn by heart puncture, the liver, spleen, kidneys and stomach were rapidly dissected, and a 1-min scintigraphic image ( $128 \times 128$  matrix) of these organs, of the tube of blood, and of the remaining carcass was obtained (static study). From the static scintigraphic image of the dissected organs and carcass, the apparent radioactivity of each of the isolated organs and remaining carcass was measured and the respective percentages of total radioactivity was calculated. The actual injected radioactivity was measured by counting radioactivity of the syringe before and after injection with a radioisotope dose calibrator (Capintec Inc., Ramsey, NJ).

Two duplicate 0.1-ml samples of each serum obtained from the heart puncture blood were subjected to two separate procedures to measure the percentage of radioactivity as antibody-bound  $^{125}\text{I}$ -ins, free  $^{125}\text{I}$ -ins,

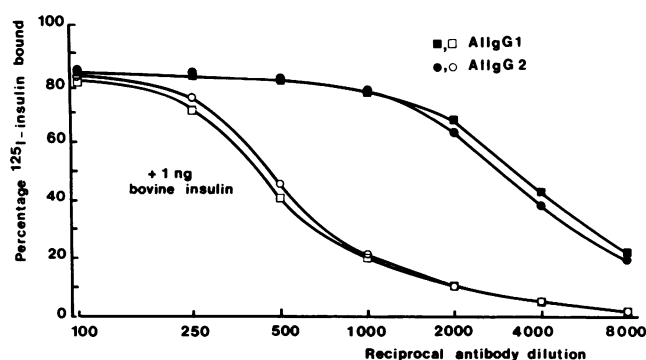


Figure 1. Titration of serial dilutions of purified guinea pig AIIgG1 (squares) or AIIgG2 (circles) in the presence of a constant amount of  $^{125}\text{I}$ -insulin, in the presence or absence of 1 ng unlabeled insulin.

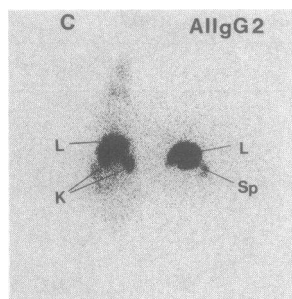


Figure 2. Scintigraph taken 3 min after i.v. injection of  $^{123}\text{I}$ -ins alone (C) or preformed IC made of  $^{123}\text{I}$ -ins and purified AllgG2. L, liver; K, kidneys; Sp, spleen.

and free  $^{123}\text{I}$ -iodide. Two 0.1-ml samples of serum were treated with 25% polyethylene glycol (PEG) to precipitate the antibody- $^{123}\text{I}$ -ins complexes (4, 18). To the supernatant an equal volume of 30% trichloroacetic acid (TCA) was added to precipitate the free  $^{123}\text{I}$ -ins. The radioactivity not precipitated by the TCA was considered free  $^{123}\text{I}$ -iodide. The other two 0.1-ml samples of serum were treated with TCA to precipitate the antibody- $^{123}\text{I}$ -ins complexes plus free  $^{123}\text{I}$ -ins. The supernate contained soluble  $^{123}\text{I}$ -iodide.

Dynamic images were analyzed as previously described (19). Briefly, regions of interest were defined over the right upper part of the liver and the lower pole of each kidney, and the heart and time-activity curves were generated. After subtraction of appropriate background, net time-activity curves were obtained. The ordinate of the heart curve was calibrated using the actual value of blood radioactivity (measured in a well type counter) on the blood sample taken at 30 min. The ordinate of the liver and kidney curves was expressed as percent of total injected and calibrated using the percentage of radioactivity in the corresponding organ measured on the static image taken at 30 min.

The digital data of each of the final three curves (60 time points per curve) were transferred to an online microcomputer (Zenith Z-100), printed on paper, and stored on floppy-disc until statistically analyzed. Time-activity curves of blood and liver were compared using a BMDP program of analysis of variance of repeated measures after log transformation of the variable. Statistical differences were determined by the Snedecor test (20).

**Clearance of  $^{123}\text{I}$ -labeled IgG1 or IgG2 of non-insulin-immunized guinea pig (NIgG1 and NIgG2).** Pure gamma globulins of non-insulin immunized guinea pig (Sigma Chemical Co., St. Louis, MO) were submitted to DEAE Sephacel anion exchange chromatography and the subclasses purified. 1 mg of each IgG subclass dissolved in 500  $\mu\text{l}$  PBS was labeled with 5 mCi Na  $^{123}\text{I}$  using lactoperoxidase and  $\text{H}_2\text{O}_2$ . The iodination mixture was then applied on a  $60 \times 1.2\text{-cm}$  6B Sepharose column equilibrated and developed with PBS. The fractions corresponding to the elution volume of an IgG standard were pooled. Four nembutal-anesthetized rats received 100  $\mu\text{Ci}$  of  $^{123}\text{I}$ -NIgG1 and a second group of four rats received the same amount of  $^{123}\text{I}$ -NIgG2. Dynamic recording and data analysis were performed as previously described for IC made of antiinsulin IgG and  $^{123}\text{I}$ -insulin.

## Results

Rats injected with guinea pig AllgG2 preincubated with  $^{123}\text{I}$ -ins sequestered virtually all of the radioactivity in the liver and spleen (Fig. 2). The total radioactivity in the circulation of these rats was extremely low. The respective percentages of AllgG2- $^{123}\text{I}$ -ins complexes, free  $^{123}\text{I}$ -ins or  $^{123}\text{I}$ -iodide (degraded insulin) in the serum at 30 min were 37, 22, and 41% (Table II). The sequestration of the radioactivity by the liver and spleen of these rats was very rapid. The scintigraph clearly demonstrates that virtually all the radioactivity was already sequestered in the liver and spleen of these rats within the first 3 min after injection. The companion scintigraph of the control rat simultaneously injected with  $^{123}\text{I}$ -ins alone demonstrates less radioactivity in the liver but in addition radioactivity in the kidneys and body of the rat is easily discerned (Fig. 2).

The sequestration of virtually all the radioactivity in the liver and spleen of the AllgG2- $^{123}\text{I}$ -ins injected rats persisted throughout the scan period and was readily apparent in the very dense scintigraph images of the dissected liver and spleen but with faint images of other organs and remaining carcass taken after the 30-min dynamic scan (Fig. 3 B). The scintigraph of the companion control rat exhibited only slight to moderate radioactivity in the liver and blood, no discernable radioactivity in the spleen, and prominent images of the carcass, kidneys, and stomach (Fig. 3 A). The radioactivity in the stomach has been demonstrated to be due to  $^{123}\text{I}$ -iodide from the degradation of  $^{123}\text{I}$ -ins (8, 19). The quantitative determination of the percentage of apparent total radioactivity in the liver and spleen of the AllgG2- $^{123}\text{I}$ -ins injected rat was 96% (Table III). In comparison the bulk of the radioactivity (75–80%) in the control rats was in the carcass.

Rats injected with AllgG1 preincubated with  $^{123}\text{I}$ -ins contained 50 times the circulating radioactivity of rats injected with AllgG2- $^{123}\text{I}$ -ins. The radioactivity in the serum of these animals was 99% precipitable by PEG and identified as AllgG1- $^{123}\text{I}$ -ins complexes (Table II). Pooling of the AllgG1- $^{123}\text{I}$ -ins complexes in the circulation is exhibited in the scintigraph taken 3 min after injection in which very dense levels of radioactivity are apparent in the heart and organs with large vascular compartments such as the liver (Fig. 4). The control rats have much less radioactivity in the heart at 3 min (Fig. 4). The circulating AllgG1- $^{123}\text{I}$ -ins complexes in these rats persist throughout the 30-min scan and are very apparent by the dense radioactivity in the carcass and in the blood removed by heart puncture (Fig. 3 C). The difference of metabolic fate of AllgG1- or AllgG2- $^{123}\text{I}$ -ins IC is further demonstrated by the time-activity curves

Table II. Radiochemical Analysis of Blood Activity

	Blood activity*	PEG			TCA	
		Ab-Ins	Ins <sup>†</sup>	I <sup>-</sup>	Ab-Ins + Ins	I <sup>-</sup>
$^{123}\text{I}$ -Ins alone (n = 5)	37.1 $\pm$ 5.3	6.6 $\pm$ 0.5	34.8 $\pm$ 1.7	58.6 $\pm$ 1.5	38.6 $\pm$ 1.3	61.4 $\pm$ 1.3
AllgG1 (n = 3)	146.1 $\pm$ 37.6	98.8 $\pm$ 0.3	0.8 $\pm$ 0.5	0.4 $\pm$ 0.2	99 $\pm$ 0.0	1 $\pm$ 0.0
AllgG2 (n = 4)	2.8 $\pm$ 2.6	36.8 $\pm$ 6.1	21.7 $\pm$ 1.7	41.5 $\pm$ 7.2	52.4 $\pm$ 4.8	47.6 $\pm$ 4.8
469 (n = 5)	16.8 $\pm$ 4.5	95.4 $\pm$ 1.1	2.4 $\pm$ 0.6	2.1 $\pm$ 0.9	96 $\pm$ 0.7	4.1 $\pm$ 0.7

Results are expressed as percent of total blood activity; mean $\pm$ SD. \* Expressed as cpm  $\times 10^{-3}$ /ml blood and normalized for total injected counts (as measured on the static frame taken at 30 min). <sup>†</sup> TCA-precipitable and PEG-soluble activity was taken as an estimate of  $^{123}\text{I}$ -insulin concentration and probably overestimates the concentration of biologically active hormone.

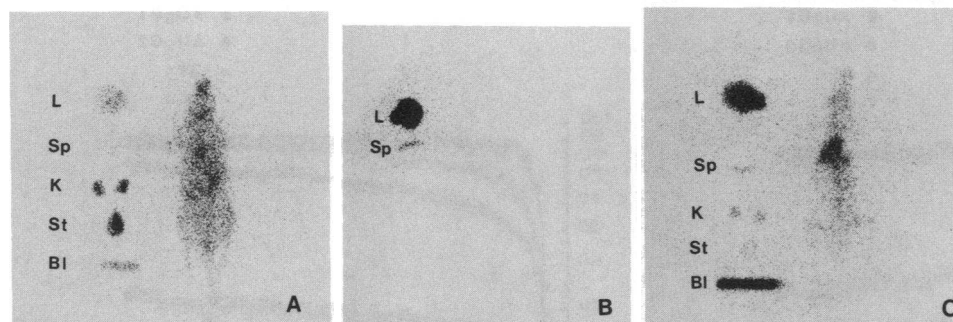


Figure 3. Scintigraph taken 30 min after i.v. injection of  $^{123}\text{I}$ -ins (A),  $^{123}\text{I}$ -ins-AllIgG2 IC (B), or of  $^{123}\text{I}$ -ins-AllIgG1 IC (C), and after dissection of the organs. Abbreviations as in Fig. 2. St, stomach; Bl, tube of blood taken by heart puncture.

of blood (Fig. 5, Table IV) and liver (Fig. 6, Table IV) generated by computer analysis of the dynamic study. These figures clearly show that AllIgG1- $^{123}\text{I}$ -ins IC remain in the blood compartment whereas AllIgG2- $^{123}\text{I}$ -ins IC rapidly leave the blood compartment and are taken up by the liver.

Pools of GPAIS (469 or 3F4) contain both isotypes of AllIgG. As expected, the blood and liver activity profiles after injection of preformed IC of 469- $^{123}\text{I}$ -ins or 3F4- $^{123}\text{I}$ -ins lie between those obtained with purified AllIgG subclasses but are closer to those obtained with purified AllIgG2.

Pretreatment with CoF did not modify the liver activity profile of rats injected with Pool 469- $^{123}\text{I}$ -ins complexes (Fig. 7;  $P = 0.645$  for identity of area under the curves and  $P = 0.2743$  for parallelism of the curves).

Previous saturation of the liver receptor compartment by 6 U regular insulin did not modify uptake of IC made of pool 469 and  $^{123}\text{I}$ -ins but markedly reduced that of  $^{123}\text{I}$ -insulin alone (Fig. 8), thus demonstrating that the mechanisms involved are completely different. On one hand, clearance of IC is independent of the presence of empty insulin receptors; on the other hand, that of insulin is essentially receptor mediated.

$^{123}\text{I}$ -labeled IgG subclasses of normal guinea pig largely remain in the blood pool. Liver activity profiles after injection of  $^{123}\text{I}$ -NIgG1 are slightly but significantly lower than after injection of  $^{123}\text{I}$ -NIgG2 (Fig. 9;  $P = 0.0054$  for identity of areas under the curves and  $P = 0.6212$  for parallelism of the curves). Statistical analysis also shows identity of the liver profiles obtained with  $^{123}\text{I}$ -NIgG1 or IC made of AllIgG1 and  $^{123}\text{I}$ -ins ( $P = 0.3977$  for identity of areas under the curves) and a marked difference for liver profiles obtained with  $^{123}\text{I}$ -NIgG2 or IC made of AllIgG2 and  $^{123}\text{I}$ -ins ( $P < 0.001$  for identity of areas under the curves).

Examination of Fig. 10 shows that free antiinsulin antibodies have the same molecular size as purified IgG in whole serum (469), purified AllIgG1, or purified AllIgG2.

Table III. Organ Distribution of Radioactivity

	Liver	Spleen
AllIgG1 ( $n = 3$ )	$32.8 \pm 0.6^\dagger$	$1.2 \pm 0.4^\dagger$
AllIgG2 ( $n = 4$ )	$92.2 \pm 4.4^\dagger$	$3.8 \pm 0.3^\dagger$
469* ( $n = 5$ )	$85.8 \pm 1.5^\dagger$	$2.1 \pm 0.3^\dagger$

Expressed as percent of total injected: mean  $\pm$  SD.

\* In the absence of effect of CoF, results obtained with 469 alone or after CoF pretreatment were pooled.

$^\dagger$  Values for AllIgG1 are statistically different from those for AllIgG2 ( $P < 0.001$ ). Liver and spleen activity after 469 differ from that after AllIgG2 ( $P < 0.05$  and  $P < 0.01$ , respectively).

Using the slow 6B Sepharose chromatographic system, preformed IC made with whole serum (469), purified AllIgG1, AllIgG2, and  $^{125}\text{I}$ -ins had an apparent molecular weight of 320,000 D, a value corresponding to dimers of IgG. When the faster FPLC system was used IC appeared much larger, corresponding to aggregates of three to more than five IgG (Fig. 11). IC had the same size whether made of whole serum or purified immunoglobulin isotypes.

Similar experiments were performed with IC made with  $^{123}\text{I}$ -insulin and the two selected human serums containing cytophilic antiinsulin IgG. Fig. 12 illustrates the liver time activity curves of rats injected with preformed IC made with 1 ml of each of the two selected serums and 100  $\mu\text{Ci}$   $^{123}\text{I}$ -insulin. With serum 1, liver activity rapidly reached circa 20% of total injected and stayed at that low level thereafter. By contrast, with serum 2, liver activity progressively increased to reach a high plateau value corresponding to circa 45% of total injected. Radiochemical analysis of blood drawn by heart puncture 30 min after IC injection showed that PEG-precipitable activity exceeded 90% of total in both cases.

The size of preformed IC made with each serum was estimated by both chromatographic methods. Using a 6B Sepharose column, IC size was intermediate between that of IgG monomers and dimers (data not shown). Using the faster FPLC system, IC were larger. Those made with serum 1 were aggregates of three IgG or less. By contrast those of the second diabetic patient were larger aggregates of up to five IgG or more (Fig. 13).

## Discussion

As previously shown,  $^{123}\text{I}$ -insulin alone is rapidly taken up by the liver (30% of total injected after 3–4 min) and the kidneys (10–15% of total injected) and rapidly degraded in both organs. For instance, in the liver, the half-life of radioactivity is  $\sim 6$  min (Fig. 8). After 30 min, liver activity is 3–5% and kidney activity is 6–8%. After  $^{123}\text{I}$ -ins degradation, free  $^{123}\text{I}$ -iodide is released into the plasma, from which it is cleared by urinary ex-

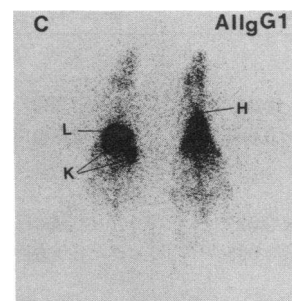


Figure 4. Scintigraph taken 3 min after i.v. injection of  $^{123}\text{I}$ -ins alone (C) or preformed IC made of  $^{123}\text{I}$ -ins and purified AllIgG1. H, heart. Other abbreviations as in Fig. 2.

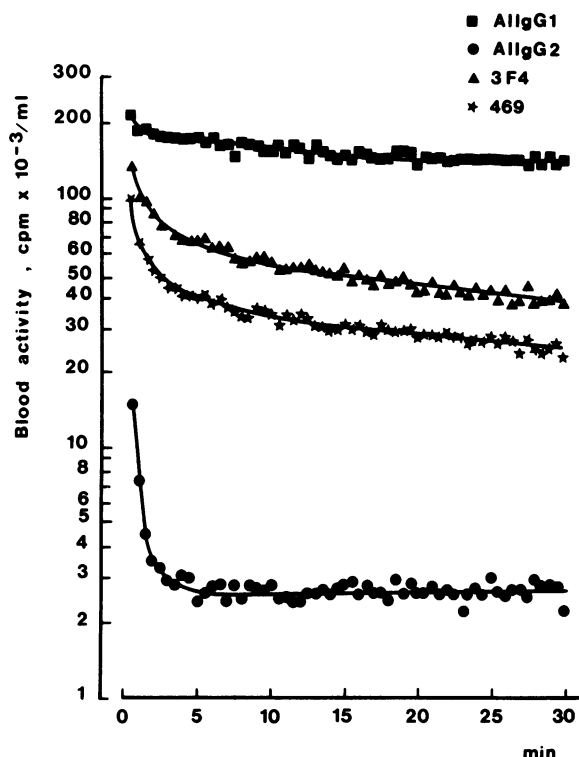


Figure 5. Profile of blood activity after i.v. injection of preformed immune complexes made up with circa 100  $\mu\text{Ci}$   $^{125}\text{I}$ -ins and purified AIIgG1 (squares), AIIgG2 (circles), serum pool 469 (stars), or 3F4 (triangles). See Table IV for statistical analysis of the data.

cretion and active transport by the gastric mucosa, salivary and thyroid glands, so that at a later time after  $^{125}\text{I}$ -ins injection, e.g. 30 min, the biodistribution of radioactivity is essentially that of iodide and characterized by dense activity in the bladder, stomach, and neck (8, 19, 21).

As shown here, the fate of antibody-bound  $^{125}\text{I}$ -ins is quite different and strongly influenced by the nature of the IgG subclass and IC size.

There is an apparent inverse relation between the level of AIIgG2 and the amount of circulating insulin antibody complexes and, conversely, a direct relation with the level of AIIgG1 in the injection bolus. On the other hand, there is a direct relationship between the amount of liver radioactivity and AIIgG2 but an inverse relationship between liver binding and AIIgG1 in the injection bolus.

Table IV. Statistical Analysis of Time Activity Curves

	<i>n</i>	Identity of means	Parallelism of the curves
Liver activity			
AIIgG2	4	$P < 0.05$	$P < 0.0001$
469	5		
AIIgG1	3	$P < 0.001$	$P < 0.0001$
Blood activity			
AIIgG2	4	$P < 0.005$	$P < 0.0001$
469	5		
AIIgG1	3	$P < 0.005$	$P < 0.0001$

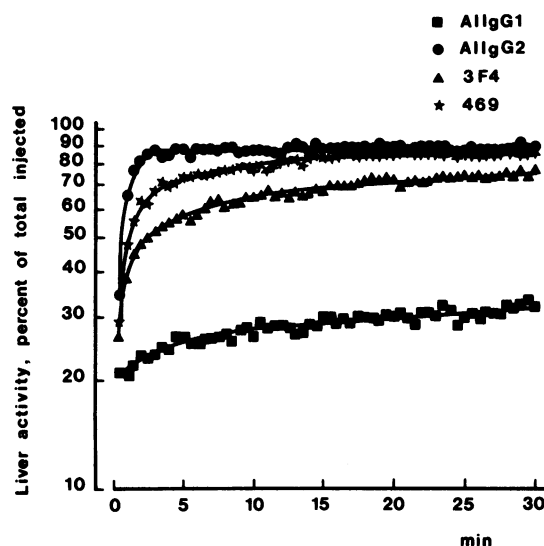


Figure 6. Liver time activity profile after i.v. injection of preformed immune complexes made up with circa 100  $\mu\text{Ci}$   $^{125}\text{I}$ -ins and purified AIIgG1 (squares), AIIgG2 (circles), serum pool 469 (stars), or 3F4 (triangles). See Table IV for statistical analysis of the data.

As previously shown with autoradiographic techniques,  $^{125}\text{I}$ -ins alone is predominantly associated with the hepatocytes whereas  $^{125}\text{I}$ -ins-GPAIS complexes are essentially associated with the Kupffer cells (21). Fig. 8 clearly shows that liver uptake of  $^{125}\text{I}$ -ins is saturable as expected for a receptor-mediated process whereas that of  $^{125}\text{I}$ -ins-GPAIS complexes is independent of the presence of free insulin receptors. These results are in good agreement with those of others who recently showed that when insulin binds to its receptor, the insulin molecule is largely buried and only a small portion remains exposed to the solvent (22, 23). This limited exposed portion reacts with very few monoclonal antiinsulin antibodies, and reacts with markedly decreased affinity when it does. When polyclonal antiinsulin antibodies

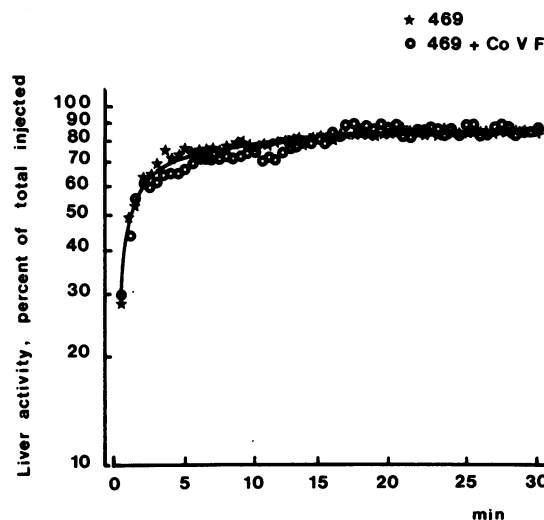


Figure 7. Liver time activity profile after i.v. injection of preformed immune complexes made up with circa 100  $\mu\text{Ci}$   $^{125}\text{I}$ -ins and serum pool 469. Control rats ( $n = 3$ ) were pretreated with saline whereas experimental rats ( $n = 2$ ) were decomplexed with 80  $\mu\text{g}$  CoF 1 h before IC injection. The two profiles are not statistically different.

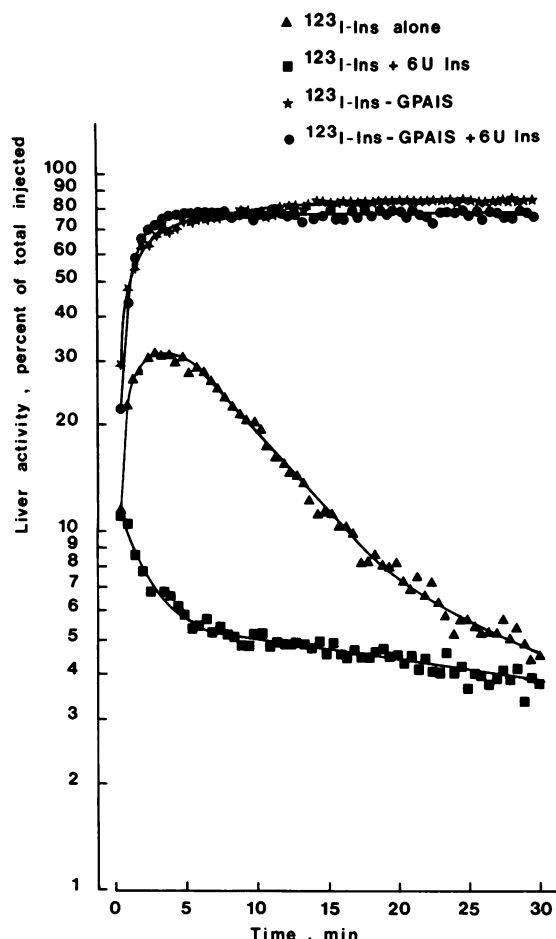


Figure 8. Liver time activity profile after i.v. injection of  $^{123}\text{I}$ -insulin alone ( $n = 10$ ) or preincubated with serum pool 469 ( $n = 5$ ). Experimental rats were pretreated with 6 U regular insulin to saturate the insulin receptor compartment before receiving  $^{123}\text{I}$ -insulin alone ( $n = 4$ ) or preformed immune complexes ( $n = 4$ ). Note that prior injection of excess unlabeled insulin markedly inhibited hepatic uptake of  $^{123}\text{I}$ -insulin but did not modify that of preformed immune complexes.

are used, binding of  $^{125}\text{I}$ -insulin to liver plasma membranes has been found enhanced and it has been speculated that antibodies are able to cross-link occupied mobile insulin receptors and that, as a result of aggregation, insulin receptors can be activated (24, 25). This tempting interpretation does not take into account two considerations. Firstly, when antibodies are polyclonal, two or possibly more epitopes (vide infra) of the insulin molecule are buried in the antigen-antibody complex. If, as discussed above, binding of one single insulin epitope to a monoclonal antibody already drastically decreases the probability of concomitant binding of insulin to its receptors, binding of two or three epitopes should further decrease or completely abolish insulin binding to its receptors. Secondly, liver plasma membranes are heterogeneous and contain not only hepatocyte membranes but also Kupffer cell membranes. The former contain insulin receptors but the latter contain receptors for Fc fragment of IgG ( $\text{Fc}\gamma\text{R}$ ), which have the capacity of binding immune complexes containing insulin. The latter possibility has recently been explored by Komori et al., who concluded that antiinsulin antibody-induced enhancement of insulin binding to liver plasma membranes was due to IC binding to  $\text{Fc}\gamma\text{R}$  (26). Thus, in vivo and

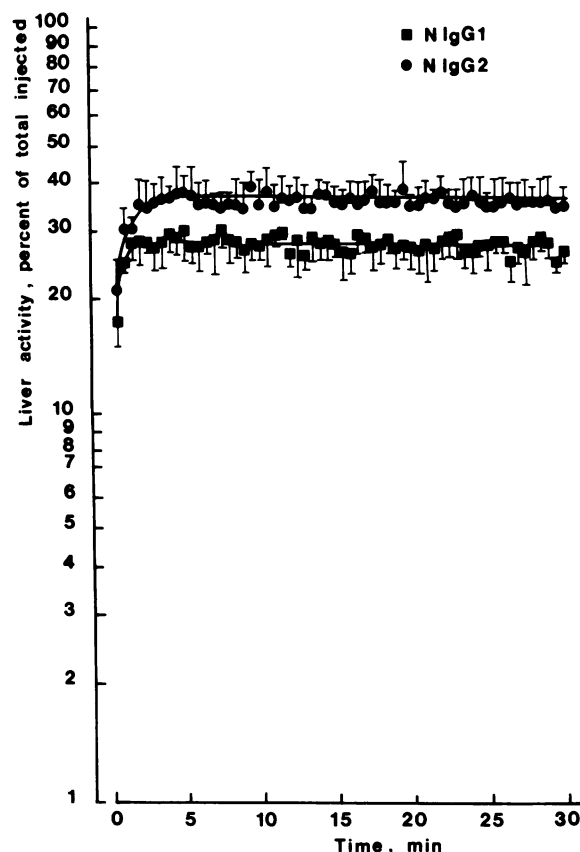


Figure 9. Liver time activity profile after i.v. injection of  $^{123}\text{I}$ -labeled NIgG1 ( $n = 4$ ) or NIgG2 ( $n = 4$ ). Liver activity was slightly but significantly higher in the presence of NIgG2 than in the presence of NIgG1. Comparison with Fig. 6 shows that NIgG1 and IC made of  $^{123}\text{I}$ -ins and specific AIIgG1 yielded superimposable liver activity profiles whereas NIgG2 and IC made of specific AIIgG2 and insulin yielded markedly different liver activity profiles.

in vitro, formation of complexes of insulin receptor-insulin-antiinsulin antibody is unlikely.

If insulin moiety of IC is not involved in the rapid and virtually total sequestration of AIIgG2- $^{123}\text{I}$ -ins complexes in the liver, the role played by the immunoglobulin moiety should be examined.

Labeled IgG1 and IgG2 of normal guinea pig are cleared at almost the same rate excluding the possibility that rapid liver uptake of  $^{123}\text{I}$ -ins-AIIgG2 IC is due to an IgG2 property independent of insulin binding and immune complexes formation.

It has previously been demonstrated that guinea pig AIIgG2 can bind complement and induce passive immune hemolysis of antigen-coated sheep red blood cells, whereas AIIgG1 only activate late components of the complement in the absence of C1, C4, and C2 fixation and are devoid of hemocytolytic properties (27-32). Because Kupffer cells possess receptors for C3b (C3bR; 33), it was reasonable to consider that complement fixation (classical pathway) could have been involved in the binding of  $^{123}\text{I}$ -ins-AIIgG2 immune complexes to macrophages in liver and spleen.

CoF, a potent activator of the alternative complement pathway was used to deplete C3. Our experiments clearly show that in CoF-treated rats, binding of immune complexes to the liver and spleen was not at all inhibited. These results agree with

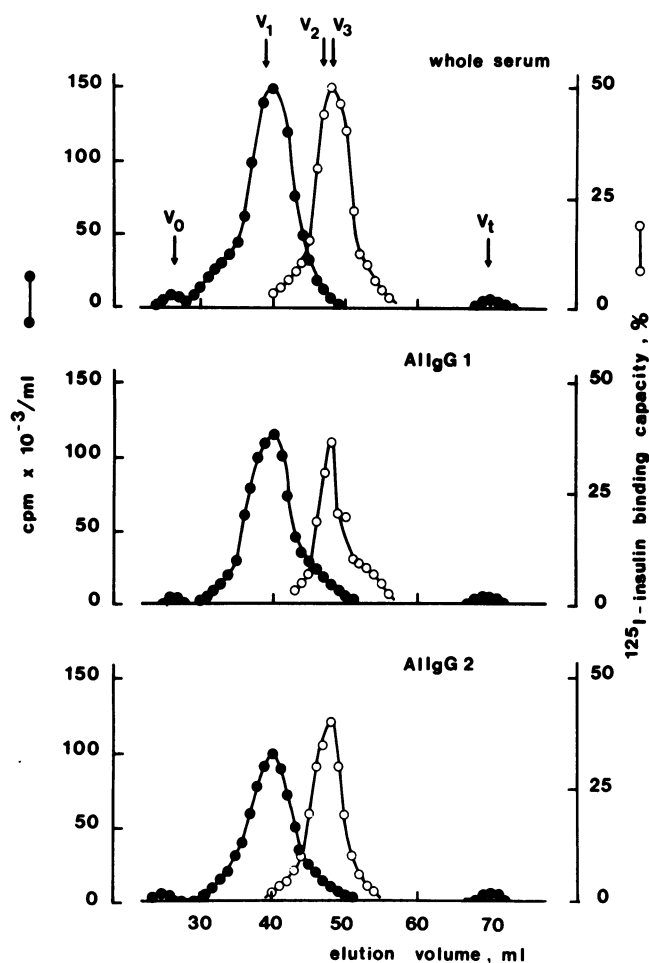


Figure 10. Elution pattern of free antibodies (open circles) or IC (solid circles) after chromatography on a  $60 \times 1.2$ -cm 6B Sepharose column. Flow rate was 4 ml/h, and 1 ml fractions were collected. IC were prepared by incubation of whole serum (469), specific AIIgG1, or AIIgG2 with  $1 \mu\text{Ci } ^{125}\text{I}$ -ins for 30 min at  $37^\circ$  immediately before chromatography. Calibration was performed using Dextran Blue ( $V_0$ ), apoferritin ( $V_1$ ),  $\beta$  amylase ( $V_2$ ), guinea pig IgG ( $V_3$ ), and lysozyme ( $V_t$ ).

those of other authors who demonstrated that the clearance of human serum albumin (HSA)-rabbit anti-HSA immune complexes was not reduced in C3-depleted mice (34). Furthermore, recent evidences indicate that complement delays clearance of large immune complexes from the blood by increasing their solubility, thereby reducing their deposition outside the reticulo-endothelial system (35). Taken together, these results would support the conclusion that complement fixation capability and C3bR on macrophages are not involved in the faster clearance of AIIgG2- $^{125}\text{I}$ -ins complexes by the liver and spleen.

Immune complex size is another factor that may influence their clearance rate. Indeed, in rats, guinea pig IgG2 monomers are cleared slowly but guinea pig IgG2 aggregates leave the vascular compartment with increasing rapidity according to lattice size, up to aggregates of 42 IgG2 (36). Actually, in our studies, IC made of  $^{125}\text{I}$ -ins-AIIgG2 were cleared as quickly as 99 mTc labeled colloid sulfur (data not shown), an agent taken up mainly by liver Kupffer cells.

Estimation of IC size is hampered by the fact that immune aggregates dissociate during the analytical step. Relatively slow

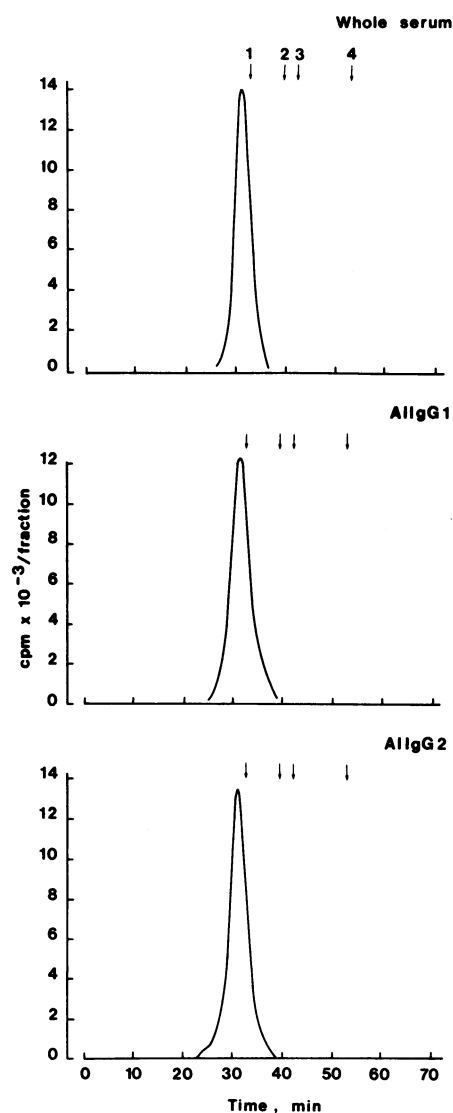


Figure 11. Elution profile of preformed IC made with whole serum (469), purified AIIgG1 or purified AIIgG2, and  $^{125}\text{I}$ -ins on a Superose 6 column. Flow rate was 0.4 ml/min. 0.2-ml fractions were collected and analyzed for activity. Calibration was performed using thyroglobulin (1), IgG (2), albumin (3), and  $^{125}\text{I}$ -insulin (4).

techniques such as ultracentrifugation (37) or 6B Sepharose chromatography (Fig. 10) yield an apparent molecular weight corresponding to that of IgG dimers. It has been postulated that dimers made of a circular complex consisting of two antibodies and two antigen molecules would be very stable and would explain the cooperative effect observed in polyclonal serum (37) or obtained by mixing two appropriate monoclonal antibodies (38). When faster analytical techniques are used, such as FPLC, the molecular weight of insulin-antiinsulin antibody IC is clearly higher than two IgG. Two theoretical models are possible. The most simple one is a linear structure in which each insulin molecule links two IgG. Alternatively, if a dimeric ring structure is the most stable unit, the existence of higher order IgG aggregates implies that rings are stacked or linked to one another either by Fc interaction (38-40) or by bridging antibodies. The latter possibility would imply that the antigenic valency of insulin is greater than two.



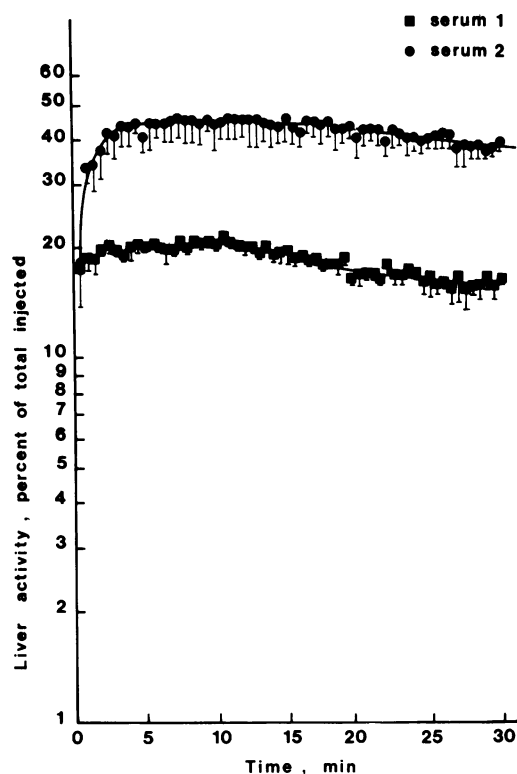


Figure 12. Liver time activity profile after i.v. injection of preformed IC made up with circa 100  $\mu\text{Ci}$   $^{125}\text{I}$ -ins and human antiinsulin serums 1 ( $n = 3$ ) and 2 ( $n = 3$ ).

Whichever its mechanism, aggregation is not the only factor responsible for rapid clearance of IC by the Kupffer cells. Indeed IC made of AIIgG1 and AIIgG2 have the same degree of aggregation, yet they are cleared at markedly different rates.

A third possible mechanism whereby AIIgG2 and not AIIgG1- $^{125}\text{I}$ -ins immune complexes are so rapidly cleared involves a particular domain of the Fc fragment, which reacts with specific Fc $\gamma$ R on the macrophages (41). It has indeed been clearly shown that guinea pig IgG2 are cytophilic for macrophages and that IgG1 are not (42–46).

As guinea pig IgG1, human IgG2, and IgG4 are not cytophilic whereas human IgG1 and IgG3 act as guinea pig IgG2 and bind to Fc $\gamma$ R. It is interesting to note that oligomeric IC made of cytophilic human antiinsulin IgG and  $^{125}\text{I}$ -insulin remain in the blood pool. By contrast, higher order aggregates formed by cytophilic human antiinsulin IgG and  $^{125}\text{I}$ -insulin are cleared by the rat macrophagic system. These results clearly show that the IgG subclass is not the only factor governing the rate at which IC are cleared from the plasma and stress the importance of the IC size.

Taken together, experiments with human and whole guinea pig serum or with purified guinea pig IgG subclasses demonstrate the interplay of two factors for the clearance of insulin-antiinsulin IgG IC. IC made of large aggregates of cytophilic IgG subclass are rapidly taken up by the Kupffer cells, resulting in insulin scavenger. All other IC, either those made of a noncytophilic IgG subclass, whatever their size or those of small size, whatever their subclass composition, remain in the plasma and result in the build-up of a potentially large pool of antibody-bound insulin.

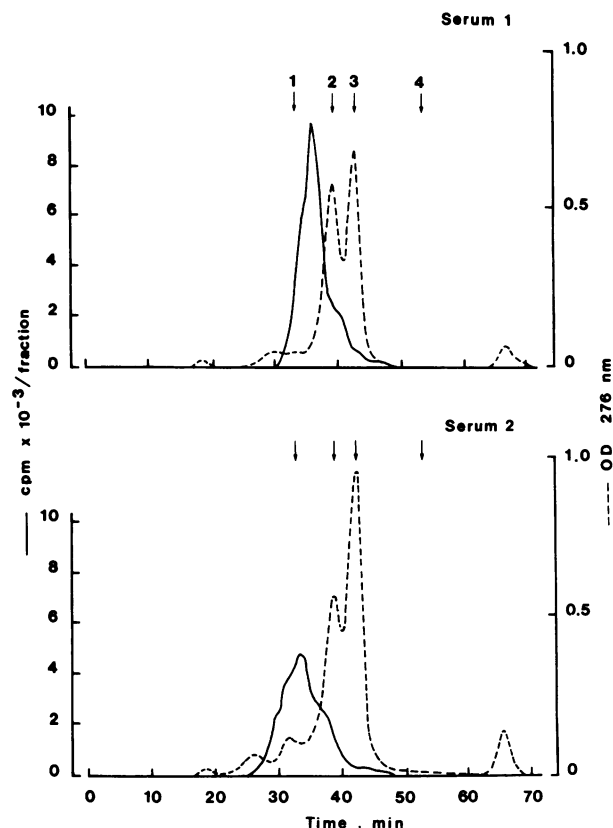


Figure 13. Elution profile of preformed IC made with human serums 1 and 2 and  $^{125}\text{I}$ -ins. Absorbance at 280 nm was measured by an on-line UV spectrophotometer. All other experimental conditions were as for Fig. 11.

## Acknowledgments

We thank Mrs. M. Hoste-Fodor for secretarial assistance and Ch. Fallais and C. Nafpliotis (Institut des Radioelements, Fleurus, Belgium) for the supply of Na  $^{125}\text{I}$  and  $^{125}\text{I}$ -insulin. We are most grateful to Dr. V. Kruse (Novo Industri AS, Copenhagen, Denmark) for stimulating discussions.

These studies were supported by grants from the Fonds de la Recherche Scientifique Medicale (Brussels, Belgium), National Institutes of Health (AM-13441), and Novo Industri AS (Copenhagen, Denmark).

## References

1. Berson, S. A., R. S. Yalow, A. Bauman, M. A. Rothshild, and K. Newerly. 1956. Insulin I-131 metabolism in human subjects. Demonstration of insulin binding globulin in circulation of insulin treated subjects. *J. Clin. Invest.* 35:170–190.
2. Kurtz, A. B., and J. D. N. Nabarro. 1980. Circulating insulin-binding antibodies. *Diabetologia.* 19:329–334.
3. Walford, S., S. P. Allison, and W. G. Reeves. 1982. The effect of insulin antibodies on insulin dose and diabetic control. *Diabetologia.* 22:106–110.
4. Heding, L. G. 1969. Determination of free and antibody bound insulin in insulin treated diabetic patients. *Horm. Metab. Res.* 1:145–146.
5. Reeves, W. G., and U. Kelly. 1980. An immunochemical method for the quantitation of insulin antibodies. *J. Immunol. Methods.* 34: 329–338.
6. Andersen, O. O., K. Brunfeldt, and F. Abildgard. 1972. A method

for quantitative determination of insulin antibodies in human plasma. *Acta Endocrinol.* 69:195-208.

7. Christiansen, A. M. 1973. Radioimmuno-electrophoresis in the determination of insulin binding to IgG. Methodological studies. *Horm. Metab. Res.* 5:147-154.

8. Sodoyez, J. C., F. Sodoyez-Goffaux, M. Guillaume, and G. Merchie. 1983. (123-I) Insulin metabolism in normal rats and humans: external detection by a scintillation camera. *Science (Wash. DC)*. 219:865-867.

9. Sodoyez, J. C., F. Sodoyez-Goffaux, M. M. Goff, A. E. Zimmerman, and E. R. Arquilla. 1975. (127-I)- or carrier-free (125-I) monoiodoinsulin. Preparation, physical, immunological, and biological properties, and susceptibility to "Insulinase" degradation. *J. Biol. Chem.* 250:4268-4277.

10. Markussen, J., and U. D. Larsen. 1980. The application of HPLC to the analysis of radio-iodinated tracers of glucagon and insulin. In *Insulin, Chemistry, Structure and Function of Insulin and Related Hormones*. D. Brandenburg and A. Wollmer, editors. W. De Gruyter, Berlin. 161-168.

11. Arquilla, E. R., and J. Finn. 1963. Insulin antibody variations in rabbits and guinea pigs and multiple antigenic determinants on insulin. *J. Exp. Med.* 118:55-71.

12. Yagi, Y., P. Maier, and D. Pressman. 1962. Two different anti-insulin antibodies in guinea pig antisera. *J. Immunol.* 89:442-451.

13. Arquilla, E. R., R. J. Dorio, and T. M. Brugman. 1976. Structural studies of insulin and insulin derivatives using various immunologic indicators and antibody populations. *Diabetes*. 25:397-403.

14. Kelso, J. M., I. Y. Tamai, M. D. Roth, I. Valdes, and E. R. Arquilla. 1980. Induction of hyperglycemia with insulin antibodies to B-chain determinants. *Diabetes*. 29:383-390.

15. Herbert, V., K. S. Lau, C. W. Gottlieb, and S. J. Bleicher. 1965. Coated charcoal immunoassay of insulin. *J. Clin. Endocrinol. Metab.* 25:1375-1384.

16. Koch, M., C. François-Gerard, F. Sodoyez-Goffaux, and J. C. Sodoyez. 1986. Semi-quantitative assessment of antiinsulin total IgG and IgG subclasses in insulin-immunized patients using a highly sensitive immunochemical micromethod. *Diabetologia*. 29:720-726.

17. Cochrane, C. G., H. J. Müller-Eberhard, and B. S. Aikin. 1970. Depletion of plasma complement in vivo by a protein of cobra venom: its effect on various immunologic reactions. *J. Immunol.* 105:55-69.

18. Desbuquois, B., and G. B. Aurbach. 1971. Use of polyethylene glycol to separate free and antibody-bound peptide hormones in radioimmunoassays. *J. Clin. Endocrinol. Metab.* 33:732-738.

19. Sodoyez, J. C., F. Sodoyez-Goffaux, S. Treves, C. R. Kahn, and R. von Frenckell. 1984. In vivo imaging and quantitative analysis of insulin-receptor interaction in lean and obese Zucker rats. *Diabetologia*. 26:229-233.

20. Dixon, W. J., editor. 1983. BMDP Statistical Software. University of California Press, Berkeley, CA.

21. Sodoyez, J. C., F. Sodoyez-Goffaux, R. von Frenckell, C. J. De Vos, S. Treves, and C. R. Kahn. 1985. Differing effects of anti-insulin serum and anti-insulin receptor serum on 123-I-Insulin metabolism in rats. *J. Clin. Invest.* 75:1455-1462.

22. Taylor, S. I., J. A. Shroer, B. Marcus-Samuels, A. McElduff, and T. P. Bender. 1984. Binding of insulin to its receptor impairs recognition by monoclonal antiinsulin antibodies. *Diabetes*. 33:778-784.

23. Maron, R., and C. R. Kahn. 1985. The insulin receptor: characterization and regulation using insulin-antiinsulin antibody complexes as a probe for flow cytometry. *J. Clin. Endocrinol. Metab.* 60:1004-1011.

24. Schechter, Y., K. J. Chang, S. Jacobs, and P. Cuatrecasas. 1979. Modulation of binding and bioactivity of insulin by anti-insulin antibody: relation to possible role of receptor self-aggregation in hormone action. *Proc. Natl. Acad. Sci. USA*. 76:2720-2724.

25. Lyen, K. R., R. M. Smith, and L. Jarrett. 1983. Differences in the ability of anti-insulin antibody to aggregate monomeric ferritin-insulin

occupied receptor sites on liver and adipocyte plasma membranes. *Diabetes*. 32:648-653.

26. Komori, K., H. Nakayama, S. Aoki, Y. Kuroda, S. Tsushima, and S. Nakagawa. 1986. Effects of antiinsulin antibody on insulin binding to liver membranes: evidence against antibody induced enhancement of insulin binding to the insulin receptor. *Diabetologia*. 29:447-452.

27. Osler, A. G., B. Oliveira, H. S. Shin, and A. L. Sandberg. 1969. The fixation of guinea pig complement by  $\gamma 1$  and  $\gamma 2$  immunoglobulins. *J. Immunol.* 102:269-271.

28. Oliveira, B., A. G. Osler, R. P. Siraganian, and A. L. Sandberg. 1970. The biologic activities of guinea pig antibodies. I. Separation of  $\gamma 1$  and  $\gamma 2$  immunoglobulins and their participation in allergic reactions of the immediate type. *J. Immunol.* 104:320-328.

29. Sandberg, A. L., B. Oliveira, and A. G. Osler. 1971. Two complement interaction sites in guinea pig immunoglobulins. *J. Immunol.* 106:282-285.

30. Götze, O., and H. J. Müller-Eberhard. 1972. Paroxysmal nocturnal hemoglobinuria. Hemolysis initiated by the C<sub>3</sub> activator system. *N. Engl. J. Med.* 286:180-184.

31. Ovary, Z., B. Benacerraf, and K. J. Bloch. 1963. Properties of guinea pig 7 S antibodies. II. Identification of antibodies involved in passive cutaneous and systemic anaphylaxis. *J. Exp. Med.* 117:951-964.

32. Corcos, J. M., and Z. Ovary. 1965. Biological properties of guinea pig anti-insulin antibodies. *Proc. Soc. Exp. Biol. Med.* 119:142-148.

33. Crofton, R. W., M. M. C. Diesselhoff-Den Dulk, and R. Van Furth. 1978. The origin, kinetics, and characteristics of the Kupffer cells in the normal steady state. *J. Exp. Med.* 148:1-17.

34. Bockow, B., and M. Mannik. 1981. Clearance and tissue uptake of immune complexes in complement-depleted and control mice. *Immunology*. 42:497-504.

35. Skogh, T., and O. Stendahl. 1983. Complement mediated delay in immune complexes clearance from the blood owing to reduced deposition outside the reticuloendothelial system. *Immunology*. 49:53-59.

36. Van Es, L. A., M. R. Daha, and A. Kijlstra. 1979. Factors influencing the endocytosis of immune complexes. In *Protides of the Biological Fluids*. H. Peeters, editor. Pergamon Press, New York. 159-162.

37. Petersen, K. G., M. J. Storch, K. Rother, T. Licht, and L. Kerp. 1985. Insulin and antiinsulin antibody interaction. Evidence for the formation of 7S and 10S structures. *Diabetes*. 34:799-802.

38. Ehrlich, P. H., W. R. Moyle, Z. A. Moustafa, and R. E. Canfield. 1982. Mixing two monoclonal antibodies yields enhanced affinity for antigen. *J. Immunol.* 128:2709-2713.

39. Møller, N. P. H., and G. Christiansen. 1983. Fc-mediated immune precipitation. III. Visualization by electron microscopy. *Immunology*. 48:469-476.

40. Møller, N. P. H., and T. S. Pedersen. 1983. Fc-mediated immune precipitation. IV. Antigen dependency and specificity. *Immunology*. 48:477-488.

41. Alexander, M. D., R. G. Q. Leslie, and S. Cohen. 1976. Cytophilic activity of enzymatically derived fragments of guinea pig IgG2. *Eur. J. Immunol.* 6:101-107.

42. Boyden, S. V. 1964. Cytophilic antibody in guinea pigs with delayed-type hypersensitivity. *Immunology*. 7:474-483.

43. Uhr, J. W. 1965. Passive sensitization of lymphocytes and macrophages by antigen-antibody complexes. *Proc. Natl. Acad. Sci. USA*. 54:1599-1606.

44. Berken, A., and B. Benacerraf. 1966. Properties of antibodies cytophilic for macrophages. *J. Exp. Med.* 123:119-144.

45. Lay, W. H., and V. Nussenzweig. 1969. CA<sup>++</sup>-dependent binding of antigen-19 S antibody complexes to macrophages. *J. Immunol.* 102:1172-1178.

46. Inchley, C., H. M. Grey, and J. W. Uhr. 1970. The cytophilic activity of human immunoglobulins. *J. Immunol.* 105:362-369.